



Programmable microencapsulation for enhanced mesenchymal stem cell persistence and immunomodulation

Angelo S. Mao^{a,b}, Berna Özkale^{a,b}, Nisarg J. Shah^{a,b,c}, Kyle H. Vining^{a,b}, Tiphaine Descombes^{a,d}, Liyuan Zhang^{b,e}, Christina M. Tringides^{a,f,g}, Sing-Wan Wong^{h,i}, Jae-Won Shin^{h,i}, David T. Scadden^c, David A. Weitz^{a,b,e}, and David J. Mooney^{a,b,1}

^aJohn A. Paulson School of Engineering and Applied Sciences, Harvard University, Cambridge, MA 02138; ^bWyss Institute for Biologically Inspired Engineering, Harvard University, Cambridge, MA 02138; ^cDepartment of Stem Cell and Regenerative Biology, Harvard University, Cambridge, MA 02138; ^dInstitute of Bioengineering, Ecole Polytechnique Fédérale de Lausanne, 1015 Lausanne, Switzerland; ^eDepartment of Physics, Harvard University, Cambridge, MA 02138; ^fHarvard Program in Biophysics, Harvard University, Cambridge, MA 02138; ^gHarvard–MIT Division in Health Sciences and Technology, Massachusetts Institute of Technology, Cambridge, MA 02139; ^hDepartment of Pharmacology, College of Medicine, University of Illinois at Chicago, Chicago, IL 60612; and ⁱDepartment of Bioengineering, College of Medicine, University of Illinois at Chicago, Chicago, IL 60612

Edited by Kristi S. Anseth, University of Colorado Boulder, Boulder, CO, and approved June 19, 2019 (received for review November 12, 2018)

Mesenchymal stem cell (MSC) therapies demonstrate particular promise in ameliorating diseases of immune dysregulation but are hampered by short in vivo cell persistence and inconsistencies in phenotype. Here, we demonstrate that biomaterial encapsulation into alginate using a microfluidic device could substantially increase in vivo MSC persistence after intravenous (i.v.) injection. A combination of cell cluster formation and subsequent cross-linking with polylysine led to an increase in injected MSC half-life by more than an order of magnitude. These modifications extended persistence even in the presence of innate and adaptive immunity-mediated clearance. Licensing of encapsulated MSCs with inflammatory cytokine pretransplantation increased expression of immunomodulatory-associated genes, and licensed encapsulates promoted repopulation of recipient blood and bone marrow with allogeneic donor cells after sublethal irradiation by a ~2-fold increase. The ability of microgel encapsulation to sustain MSC survival and increase overall immunomodulatory capacity may be applicable for improving MSC therapies in general.

biomaterials | regenerative medicine | MSC | microfluidics | immune modulation

Mesenchymal stem cells (MSCs) have generated significant interest as potent immune modulators capable of ameliorating a number of disease states, including graft-versus-host disease (1, 2), solid organ and graft rejection (3, 4), and inflammatory bowel disease (5). However, translation of preclinical results to the clinic has been challenging. A number of discrepancies likely hamper the clinical efficacy of MSC therapies, including the relatively larger dosage received by animal models compared with human subjects, potential alloimmune reactions against donor MSCs, and suboptimal phenotype of MSCs used in clinical settings (6, 7). Moreover, MSC administration is characterized by a short in vivo persistence time, during which infused cells transiently affect the host environment via paracrine factors (8, 9). As such, development of strategies that can increase MSC in vivo persistence without reducing their fitness may improve MSC therapies in general and ease translation into clinical settings.

One promising strategy to improve MSC therapies is biomaterial encapsulation. Various biomaterial formulations have been shown to support and direct MSC phenotype, in both preclinical and clinical settings (10–15). However, these strategies generally involve encapsulation of MSCs in bulk hydrogels that preclude their administration in an intravenous (i.v.) context, which is the preferred clinical route of delivery (7). Furthermore, the diffusion of relevant biomolecules may be hampered by the relatively large volume of hydrogel (16). A microfluidic approach to encapsulate MSCs into a thin, conformal coating of alginate material, termed microgels, has decreased the size of encapsulates, improved diffusional transport, and increased in vivo persistence

after i.v. administration (17), but the therapeutic efficacy of this approach has been unexplored.

Here, we test the hypothesis that simple modifications to alginate microgels encapsulating MSCs, namely secondary cross-linking and increasing cellularity of encapsulates, can substantially augment in vivo persistence without compromising the diffusion of secreted factors, and thereby boost overall MSC immunomodulatory function. We used a microfluidic approach to encapsulate cells to permit i.v. delivery. Spheroid formation and secondary cross-linking of hydrogel have been shown separately to increase transplanted cell survival (18, 19). We tested the compatibility of these modifications with microgel encapsulates, and subsequently their effect on in vivo persistence, with or without hostile host immune activity. Finally, a bone marrow (BM) transplant model was chosen to test the immunomodulatory function of encapsulated MSCs. BM transplant is a potentially curative treatment for hematological malignancies, but allogeneic graft failure is a significant complication, and likely to be of increasing importance due to the wider adoption of

Significance

Mesenchymal stem cell (MSC) therapies have shown strong preclinical promise, particularly in ameliorating diseases of immune dysregulation. However, these results have largely failed to demonstrate efficacy in clinical settings, likely due to large dosages necessitated by the short residence time of infused cells, suboptimal cell phenotype, and immune rejection. We demonstrate that a microfluidic-based biomaterial encapsulation approach can increase in vivo residence time after intravenous (i.v.) delivery by more than an order of magnitude. Encapsulated cells up-regulated immunomodulatory genes upon exposure to inflammatory cytokines and promoted engraftment of major histocompatibility complex (MHC)-mismatched donor cells in a bone marrow transplant model. The ability to retain i.v. infused MSCs for longer durations may be broadly applicable toward improving MSC therapies.

Author contributions: A.S.M., N.J.S., J.-W.S., D.T.S., D.A.W., and D.J.M. designed research; A.S.M., B.Ö., N.J.S., K.H.V., T.D., C.M.T., and S.-W.W. performed research; A.S.M. and L.Z. contributed new reagents/analytic tools; A.S.M., B.Ö., K.H.V., T.D., C.M.T., and S.-W.W. analyzed data; and A.S.M. and D.J.M. wrote the paper.

The authors declare no conflict of interest.

This article is a PNAS Direct Submission.

Published under the PNAS license.

¹To whom correspondence may be addressed. Email: mooneyd@seas.harvard.edu.

This article contains supporting information online at www.pnas.org/lookup/suppl/doi:10.1073/pnas.1819415116/-DCSupplemental.

Published online July 16, 2019.

HLA-mismatched grafts and reduced intensity conditioning (20, 21). MSC administration has attracted attention in this context, and while the safety profile of this approach is established, its efficacy remains in question (22).

Results

Fabrication and Culture of Encapsulated Cells. A mouse mesenchymal stromal cell (mMSC) line was encapsulated into microgels using a flow-focusing microfluidic device, as described earlier (17) (Fig. 1A). As the ability to cryopreserve and store encapsulated cells would expedite their use in preclinical and clinical settings, microgel size and viability of encapsulated cells in freeze-thawed encapsulated cells were quantified. Microgel morphology and size appeared unchanged by the freeze-thaw process (Fig. 1B and *SI Appendix, Fig. S1A and B*). Thawed cells exhibited a similar, high viability as freshly encapsulated cells (Fig. 1C). Thawed cells were amenable to continued culture and underwent proliferation over the course of 2 d of culture, forming small multicellular cell clusters within a thin layer of alginate (Fig. 1D and E).

As the stability of the hydrogel capsule could limit cell durability following transplantation, the ability of poly-D-lysine (PDL) coating, followed by subsequent exposure to soluble alginate to form alginate-PDL-alginate (APA) constructs, was explored. Exposure of cell-encapsulating microgels to PDL reduced overall microgel diameter, due to contraction of the initial gel coating around cell surfaces (Fig. 1F). APA treatment also reduced the proliferation of encapsulated cells compared with untreated microgels, likely due to greater difficulty for cells to remodel substrates that had received secondary cross-linking (Fig. 1E). Microgel size reduction was found to vary as a function of PDL

concentration, and this behavior was observed in both microgels with an initial diameter of 30 μm as well as larger 50- μm microgels. The medium in which PDL exposure was performed impacted microgel shrinkage. In fetal bovine serum (FBS)-supplemented Dulbecco's modified Eagle's medium (DMEM), higher PDL concentrations were required to reduce microgel size, compared with PDL exposure in a protein-free Hepes buffer (Fig. 1G). The fold change in microgel size appeared to be independent of the initial microgel size (*SI Appendix, Fig. S1C*) and occurred within minutes (*SI Appendix, Fig. S1D*).

To assess how PDL treatment might affect diffusion of soluble factors in the hydrogel coating, a variation of fluorescence recovery after photobleaching was performed using fluorescently labeled soluble dextran molecules of different molecular weights within the gels as model molecules (*SI Appendix, Fig. S1E*). APA modification did not preclude diffusion of any of the dextrans tested, and bleached areas all eventually recovered their fluorescence. PDL treatment did not significantly affect the half-life recovery of the dextrans, except in the case of dextrans of the highest molecular weight tested (500 kDa), in which half-life increased by <25% (Fig. 1H).

Finally, the viability of mMSCs encapsulated in APA microgels as well as the ability of APA treatment to retain mMSCs within their encapsulation were assessed. All encapsulated mMSCs exhibited high viabilities, with no significant differences between APA-treated and untreated encapsulates (Fig. 1I). mMSC egress from or retention within microgels was assessed by embedding encapsulates into a collagen hydrogel, to emulate transplantation into an *in vivo* environment. Nearly 90% of mMSCs were fully retained inside APA microgels, with small fractions producing extrusions or egressing into the surrounding matrix, compared with less than 20% of untreated controls fully retained inside microgels. Encapsulates that were exposed to 30 mM calcium to induce stronger calcium-mediated cross-linking of alginate also exhibited lower levels of egress than untreated encapsulates (Fig. 1J).

In Vivo Residence Time of Encapsulated Cells. We next tested how increased cellularity and PDL treatment would affect residence time of *i.v.* infused mMSCs. mMSCs were transduced with a firefly luciferase reporter and subsequently injected bare, encapsulated without further treatment, with subsequent culture, with APA treatment, or with culture and APA treatment as multicellular APA (MAPA) microgels. Recipient animals were imaged 2 h after injection and daily for 5 d afterward (Fig. 2A), and half-life of luminescent signal was calculated from an exponential decay curve fit (Fig. 2B–D).

Consistent with prior findings (23), both encapsulated and bare mMSCs were found predominantly in the lungs after injection (*SI Appendix, Fig. S2A and B*). Bare mMSCs were rapidly cleared with a half-life of less than 2 h, subsequent to the initial time point, which was taken at 2 h after injection. Further time points confirm the rapid, exponential decay of bare cells (*SI Appendix, Fig. S2C*). However, encapsulation into microgels significantly increased the cellular half-life. Culturing encapsulated mMSCs to generate multicellular clusters before transplantation did not further increase half-life (Fig. 2B). However, encapsulated cell clusters treated with PDL to form MAPA microgels led to a significantly higher residence time after injection (Fig. 2C and *SI Appendix, Table S1*). The increased residence time was likely not a result of increased cell number, as equal numbers of cells were administered in MAPA and single-cell groups, and recipient mice exhibited similar luminescent signals (*SI Appendix, Fig. S2D*). The resulting half-life of more than 50 h constitutes a roughly 5-fold increase over untreated microgels, and more than an order of magnitude increase over bare cells. To determine whether this approach was extensible to other modalities of modifying gel cross-linking, multicellular microgels were treated with calcium in place of PDL. Similar to results with PDL, calcium treatment of multicellular microgels significantly increased residence time compared with untreated microgels, but the magnitude of this effect was lower than in MAPA microgels (Fig. 2D). Next, the ability of MAPA mMSCs to be cryopreserved was tested. Freeze-thawed MAPA encapsulates

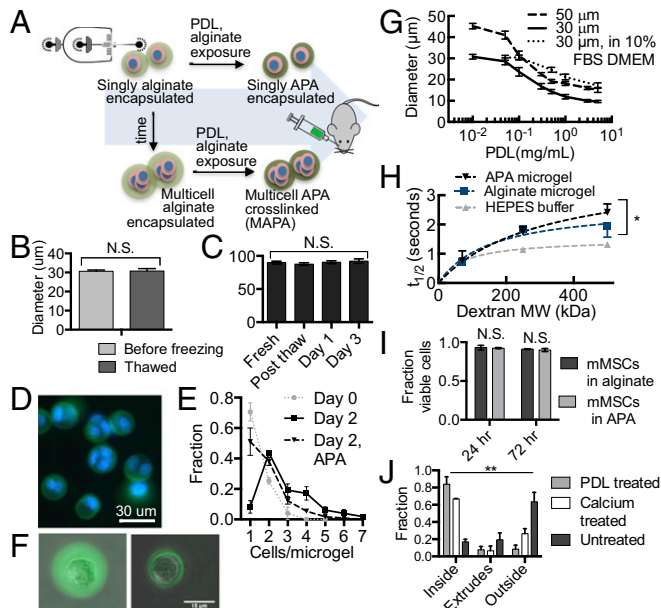


Fig. 1. Encapsulation of mMSCs into alginate and alginate-PDL-alginate (APA) microgels. (A) Schematic of encapsulation and subsequent treatments. Diameters (B) and viability (C) of mMSC-encapsulating microgels before and after cryopreservation (2-tailed Student's *t* test or χ^2 test). (D) Encapsulated mMSCs after 2 d of culture. Green, alginate; blue, DAPI. (E) Distribution of cells per microgel at day 0 and day 2. (F) Fluorescent and bright-field overlay of encapsulated cell before and after PDL exposure. Green, alginate. (G) Microgel diameter after exposure to 5-kDa PDL as a function of PDL concentration in serum-free buffer, except where noted. (H) Half-life of fluorescent recovery of dextrans after photobleaching. (I) Encapsulated mMSCs viability with and without PDL treatment (χ^2 test). (J) Fraction of mMSCs that remained inside, produced extensions out of, or egressed from calcium-treated and APA encapsulates. Error bars show SD from 2 independent experiments (χ^2 test). * $P < 0.05$; ** $P < 0.01$. N.S., not significant.

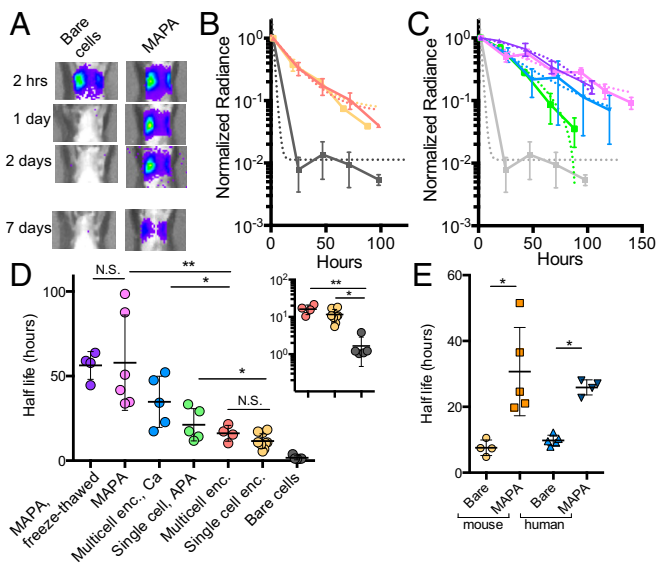


Fig. 2. In vivo persistence of infused mMSCs with different encapsulation parameters. (A) Luminescent signal of bare and MAPA encapsulates in B6 recipient mice postinjection. Total radiance over time normalized to initial 2-h signal of (B) bare mMSCs (Bare cells), mMSCs encapsulated in alginate (Single cell enc), or mMSCs encapsulated in alginate followed by proliferation (Multicell enc); and (C) mMSCs encapsulated followed by APA (Single cell, APA), by proliferation and calcium (Multicell enc., Ca), and by proliferation and APA (MAPA). Normalized radiance of bare mMSCs included for comparison (faded gray). The colors in B and C match x-axis labels in D. (D) Half-life of signal from infused mMSCs. See *SI Appendix, Methods*. Bare cells, or microgels with single or multiple cells, were subject to a 1-way ANOVA followed by multiple comparisons (*Inset*). Other significant testing was conducted using a 2-way ANOVA with multiple comparisons on ranked observation or 2-way Mann–Whitney tests. (E) Half-life of primary bare cells and MAPA encapsulates. * $P < 0.05$; ** $P < 0.01$. N.S., not significant.

exhibited similar gross morphology and diameters as fresh MAPA encapsulates (*SI Appendix, Fig. S2 E and F*) and high viability, although viability was slightly lower (80%) after 3 d of culture (*SI Appendix, Fig. S2 G*), likely due to the relative inability of cells to proliferate in APA treatment encapsulates (Fig. 1E). Furthermore, cryopreserved MAPA encapsulates administered i.v. into recipient mice immediately after thawing exhibited similar levels of improved survival as fresh MAPA-encapsulated mMSCs (Fig. 2 C and D), with an average half-life of 56 h. Finally, MAPA encapsulation was found to significantly increase residence time of primary mMSCs as well as primary human MSCs (hMSCs) (Fig. 2E and *SI Appendix, Fig. S2 H*).

To investigate the mechanism of MAPA-mediated prolonged residence time, collagen I deposition and oxygen tension were assessed, as hypoxia and matrix deposition have been implicated in the phenotypic differences between spheroids and single cells (24). Multicellular encapsulates produced higher levels of collagen I than single-cell encapsulates (*SI Appendix, Fig. S2 I and J*). Significantly lower oxygen tension was observed in multicellular encapsulates, compared with single-cell encapsulates, but aggregates of cells with dimensions typical of spheroids ($>100 \mu\text{m}$) experienced much greater hypoxia than encapsulates (*SI Appendix, Fig. S2 K and L*).

Host Physiological Response to Administered Cells. Next, the physiological response to infused encapsulated cells was assessed. Recipient animals were killed 2 wk after injection of MAPA mMSCs, and explanted lungs were stained with hematoxylin and eosin (H&E) and Masson's trichrome (Fig. 3A). Regions around microgels demonstrated a lack of cellular infiltration and fibrotic deposition. To assess host response at earlier time points, lungs were explanted 4 d after injection. Immunostaining for CD68 and C3 revealed the presence of macrophages and complement activation, respectively, in

the vicinity of MAPA mMSCs (Fig. 3 B and C). To assess whether encapsulates may adversely affect pulmonary physiology, an Evans blue albumin dye assay was performed to quantify pulmonary vascular permeability (Fig. 3D). Only injection with lipopolysaccharide, but not with either APA encapsulated or bare mMSCs, led to a significant increase in vascular permeability.

To assess whether macrophages and complement played a role in clearance, recipient mice were injected with either clodronate liposomes or cobra venom factor (CVF) before transplants. Clodronate administration reduced the relative fraction of circulating CD11b⁺ cells (*SI Appendix, Fig. S3 A*), while CVF diminished serum C3 activation (*SI Appendix, Fig. S3 B*) compared with wild-type (WT) mice. Bare and MAPA mMSCs were administered to mice that had received clodronate liposomes or CVF, and their luminescent signal was measured over time. When bare mMSCs were suspended in a protein-free HEPES buffer, neither clodronate nor CVF appeared to affect the already short mMSC half-life. MAPA mMSCs exhibited similar, long half-lives in clodronate or CVF-treated mice, compared with WT mice (Fig. 3E and *SI Appendix, Fig. S3 C*).

To test the ability of MAPA encapsulation to protect mMSCs from immune clearance, an innate immune-mediated response directed locally at MAPA encapsulates was generated by incubating MAPA-encapsulated and bare mMSCs in FBS-containing medium before injection. Adsorbed xenogenic proteins have been shown to promote foreign body responses by increasing macrophage and complement attachment (25). Unencapsulated cell half-life appeared unchanged, at ~ 3 h. The half-life of MAPA-encapsulated mMSCs in both WT and CVF-treated mice was reduced to roughly 15 h. In this setting, clodronate administration, but not complement inactivation, significantly increased the half-life of MAPA-encapsulated mMSCs (Fig. 3F and *SI Appendix, Fig. S3 D*). This finding suggests that macrophages respond to adsorbed xenogenic proteins with increased clearance of MAPA encapsulates, although MAPA encapsulation still provided substantial protection to the cells.

Next, the ability of encapsulation to extend the half-life of mMSCs in recipients with a preexisting alloresponse against donor cells was tested, as MSC therapies will often be dosed multiple

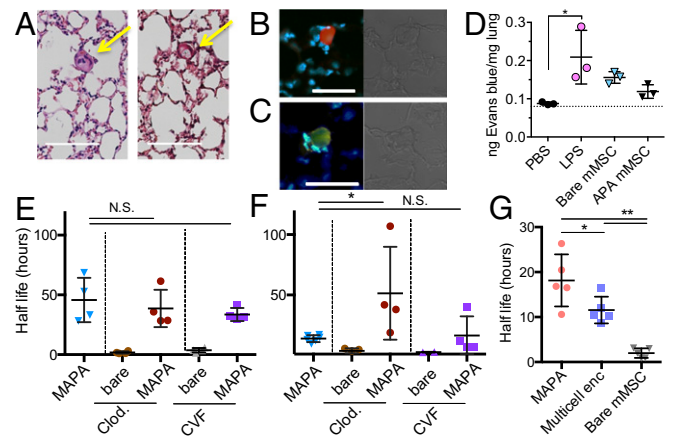


Fig. 3. Interaction of host immunity and infused mMSCs. (A) H&E (Left) and Masson's trichrome (Right) stains of lungs explanted from recipient mice 2 wk after injection of mMSCs encapsulated in APA microgels. Fluorescent (Left) and transmitted light images (Right) of mMSC-encapsulating APA microgels explanted and stained for C3 protein (B) or CD68 (C) and DAPI. Green, alginate; red, C3; yellow, CD68. (D) Evans blue extravasation in pulmonary vasculature permeability. One-way ANOVA, Sidak's multiple-comparison test. Half-life of signal from mice that had received infused mMSCs in HEPES buffer (E) or complete DMEM (F), with or without clodronate or CVF administration. (G) Half-life of mMSC in primed B6. mMSC were injected either bare, in multicellular encapsulates (multicell enc.), or as MAPA encapsulates. Two-tailed Student's *t* test in E, Mann–Whitney test in F, and Kruskal–Wallis with multiple comparisons in G. * $P < 0.05$; ** $P < 0.01$. N.S., not significant.

times. To elicit a preexisting memory T-cell response, B6 mice received an initial injection of mMSCs, which were of BALB/c origin (*SI Appendix, Fig. S3E*). An in vivo cytotoxicity assay performed 2 wk later using CFSE-labeled BALB/c splenocytes indicated that a memory T-cell response against cells of BALB/c background had indeed been elicited (*SI Appendix, Fig. S3 F and G*). In these primed mice, encapsulation significantly increased the half-life of subsequently injected mMSCs compared with bare cells, albeit to lower levels than in naive WT mice (*Fig. 3G and SI Appendix, Fig. S3H*). MAPA modification also significantly increased mMSC half-life compared with allogeneic mMSCs in unmodified microgels.

Expression of Hematopoietic and Immunomodulatory Genes. As the mechanism of MSC therapeutic efficacy has been linked to production of immunomodulatory proteins and cytokines (26, 27) and support of hematopoiesis (28, 29), gene expression of mMSCs with or without MAPA encapsulation was measured using real-time PCR. A set of genes related to immunomodulatory factors associated with MSCs were chosen (Il-6, Il-10, Ccl2, Ccl5, TGF- β , Nos-2, TSG-6, mPGES-2, Cox-2), as well as 3 proteins involved in MSC regulation of hematopoietic stem cells (SCF, TPO, CXCL12) (*SI Appendix, Table S2*). MAPA encapsulation led to differences in gene expression compared with control cells grown on tissue culture polystyrene. Ccl5, CXCL12, SCF, and TPO were expressed at lower levels, whereas encapsulation increased levels of Il-10, Il-6, Cox-2, TGF- β , and TSG-6. (*Fig. 4A*). The impact of APA treatment on gene expression of encapsulated cells was also assessed. Compared with multicellular encapsulates without APA treatment, MAPA encapsulates expressed lower levels of CXCL12 and SCF, and higher levels of Cox2 (*Fig. 4B*).

Licensing MSCs by exposure to inflammatory cytokines has been shown to boost their efficacy by up-regulating expression of immunomodulatory factors (30). To test licensing in MAPA mMSCs, gene expression was assessed in mMSCs exposed to TNF α and IFN- γ . Exposure boosted expression of certain genes in both control and MAPA mMSCs. In particular, Ccl2, Ccl5, and Nos-2 levels increased by more than 2 orders of magnitude in both encapsulated cells and bare controls (*Fig. 4C and SI Appendix, Table S3*). Although significant differences in gene expression existed between mMSCs licensed on tissue culture polystyrene and in MAPA encapsulates, overall levels of gene expression correlated closely upon licensing (*Fig. 4C and SI Appendix, Fig. S4A*). The influence of encapsulate substrate properties on licensing was also assessed. Fold change in gene expression upon licensing of multicellular encapsulates without APA treatment and of MAPA encapsulates closely correlated (*Fig. 4D*), although the overall increase in gene expression was more pronounced in multicellular encapsulates, compared with MAPA mMSCs (*SI Appendix, Fig. S4B*). Finally, to assess the extent to which cryopreservation may impact the responsiveness of mMSCs to licensing, gene expression

between fresh and cryopreserved MAPA encapsulates was compared. The fold change of gene expression of the 2 groups strongly correlated, suggesting that the freeze–thaw process preserved the cells' responsiveness to licensing (*Fig. 4E*).

MAPA Encapsulation with Licensing Boosts Allogeneic Engraftment.

To test the immunomodulatory effect of MAPA mMSCs in vivo, encapsulates were administered in a competitive BM transplant model. WT CD45.2 BALB/c mice were sublethally irradiated before receiving a transplant consisting of an equal mixture of congenic and allogeneic donor BM, derived from B6-GFP mice and CD45.1 BALB/c mice, respectively. Immediately after donor BM injection, mMSCs either with or without MAPA encapsulation, as well as with or without licensing, were introduced into recipient mice (*Fig. 5A*).

Blood and BM from recipient mice were analyzed after 9 d with flow cytometry to determine engraftment of allogeneic and congenic donor cells (*Fig. 5B and SI Appendix, Fig. S5*). Only coadministration of donor BM with licensed MAPA mMSCs resulted in a significantly higher fraction of allogeneic CD45 cells, relative to total donor-derived CD45 cells, in both blood and BM, compared with controls in which donor BM was injected with buffer only (*Fig. 5 C and D*). Whereas only 19% of BM was composed of allogeneic cells in control mice, mice that had received coinjection of MAPA mMSCs had an average 50% increase in repopulation with allogeneic cells. The increase in allogeneic-derived cells in the blood was even higher, with an average increase from 11% to more than 36%. To test interaction between encapsulation and licensing, a 3-way ANOVA was conducted on data from pooled blood and BM engraftment. A significant main effect was found for encapsulation, as well as an interaction between encapsulation and licensing (*SI Appendix, Table S4*). The durability of mMSCs was then correlated with blood and BM allogeneic engraftment. Luminescent signal from mMSCs at 1 d after administration demonstrated a significant positive correlation with blood and BM engraftment (*Fig. 5 E and F*).

Finally, the abilities of primary mMSCs and hMSCs to increase allogeneic engraftment were tested. Donor BM administered with licensed MAPA-encapsulated primary mMSCs increased allogeneic engraftment compared with administration with a buffer control or licensed, bare primary mMSCs (*Fig. 5G*). Administration with licensed MAPA-encapsulated primary hMSCs did not increase allogeneic engraftment compared with a buffer control but did produce higher levels of allogeneic engraftment compared with bare, licensed hMSCs (*Fig. 5H*).

Discussion

Methods to improve MSC therapies are currently of intense interest, due to the promise of MSC therapies to ameliorate a number of immune and inflammatory-related disease and injury states. Here, we show that appropriate encapsulation into alginate

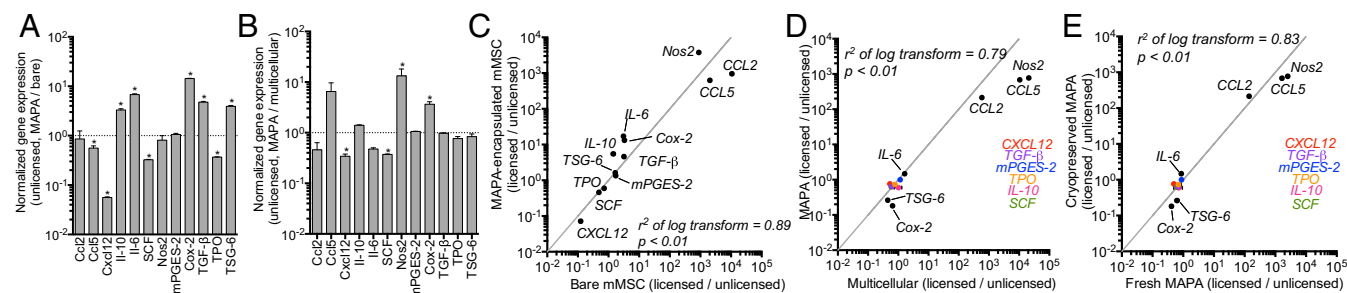


Fig. 4. Effects of encapsulation and licensing on mMSC gene expression. Gene expression in MAPA mMSCs, normalized to mMSCs on tissue culture plastic (*A*) and in encapsulates without APA treatment (*B*), all without cytokine licensing. (*C*) Gene expression of licensed bare mMSCs versus licensed MAPA-encapsulated mMSCs, both normalized to unlicensed mMSCs grown on tissue culture plastic. (*D*) Gene expression of licensed multicellular encapsulates, normalized to unlicensed, compared with licensed MAPA encapsulates, normalized to unlicensed. (*E*) Gene expression of MAPA mMSCs licensed immediately after fabrication, normalized to unlicensed, compared with MAPA mMSCs licensed after cryopreservation, normalized to unlicensed. r^2 in *C–E* calculated from Pearson's correlation of log transforms. Normality assessed using the D'Agostino–Pearson test. Gray line shows $x = y$ for reference. * $P < 0.05$.

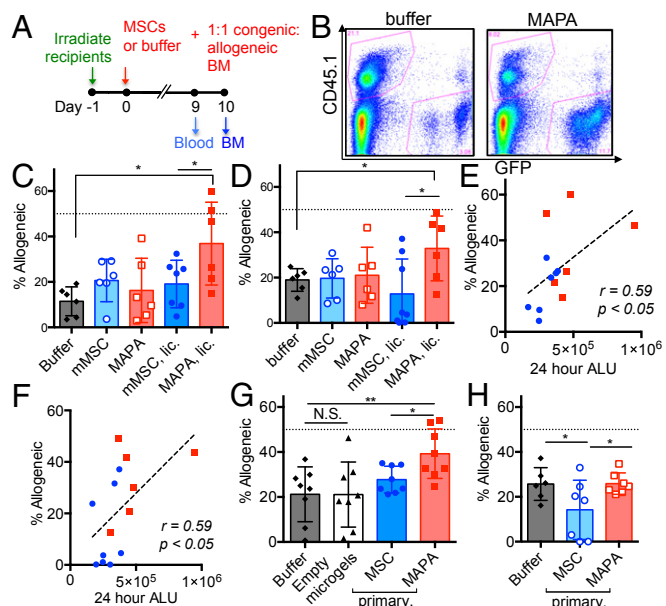


Fig. 5. Effects of MAPA-mMSC on allogeneic engraftment. (A) Schema of competitive allogeneic transplant. All animals received a 1:1 mixture of congenic and allogeneic donor BM cells. (B) Representative flow cytometry plots from BM at 9 d. (C) Percent allogeneic cells in blood (C) and femur (D) in mice that had received donor BM cells with buffer and various MSC conditions. Student's *t* test with Welch's correction. Correlation between luminescent signal from licensed bare or MAPA mMSCs at 24 h and percent allogeneic cells in blood (E) and femur (F) at 9 d using the nonparametric Spearman test. The dashed line shows best-fit linear regression and was not used for statistical testing. (G) Percent allogeneic cells in femur in mice that had received donor BM cells with buffer; empty APA microgels; and licensed primary mMSC, bare or MAPA. One-way ANOVA with Sidak's multiple comparisons. (H) Percent allogeneic cells in femur in mice that had received donor BM cells with buffer, licensed bare primary hMSCs, and licensed MAPA primary hMSCs. One-way ANOVA with Fisher's least significance difference. **P* < 0.05; ***P* < 0.01. N.S., not significant.

microgels dramatically extends in vivo persistence of i.v. injected mMSCs, with multicellular cell clusters encapsulated in APA microgels prolonging the half-life by more than an order of magnitude. MAPA encapsulation resulted in longer in vivo persistence relative to unencapsulated cells even in the presence of macrophage and adaptive immune-mediated immune clearance, while permitting licensing of encapsulated cells by inflammatory cytokines. Finally, licensed MAPA mMSCs resulted in greater repopulation of blood and BM with allogeneic donor cells when infused with donor BM in a competitive transplant.

Using a microfluidic approach, mMSCs could be encapsulated into alginate microgels that enabled subsequent culture and cell proliferation, as well as secondary cross-linking. Cell clusters could be induced to form from initial single cells simply via subsequent culture. Importantly, these encapsulates, both with and without MAPA treatment, could be readily cryopreserved with conventional cryopreservation techniques. Moreover, MAPA encapsulates used immediately after retrieval from cryopreservation demonstrated the same level of increased in vivo persistence as fresh MAPA encapsulates, and possessed similar responsiveness to inflammatory cytokines licensing. These results accord with studies using larger cell encapsulates (31). Cryopreservation is crucial for MSC therapies for acute injuries and is of considerable interest from a commercial standpoint.

The results here demonstrate that simple approaches to modify cellularity and secondary cross-linking of encapsulates can increase half-life of infused encapsulated cells in the context of i.v. administration, the clinically preferred delivery method

(7). The 2 advances described here, polylysine cross-linking and cell cluster formation, were shown to separately improve transplanted cell survival in other contexts (18, 19, 32). The reduction of microgel diameter upon polylysine treatment is consistent with prior observations and may be due to neutralization of negative charges of the alginate polymer (33). The increased half-life seen here with PDL treatment may stem from reduced cell egress and subsequent exposure to hostile mechanical and immune forces. This effect was not limited to PDL treatment, as a calcium treatment similarly reduced cell egress and increased MSC half-life, suggesting that increasing microgel mechanical strength in general augments cellular persistence. Gel degradation is unlikely to contribute substantially to cellular clearance, as cell-free, unmodified microgels have previously been shown to clear with a half-life of 141 h, much larger than the 12-h half-life observed with the same formulation of microgels, and would be expected to increase with further cross-linking (17).

Multicellularity and PDL cross-linking combined produced the greatest increase in in vivo MSC persistence. MSC spheroids exhibit higher survival when transplanted, with mild hypoxia and enhanced extracellular matrix secretion implicated in induction of prosurvival genes (19, 24, 34). Both these factors were observed in cell clusters here, although the degree of hypoxia was much milder than in large spheroids. This suggests that the increased survival in these smaller cell clusters may exploit similar mechanisms. However, as multicellularity alone without encapsulation in calcium or PDL-cross-linked microgels appeared to have no effect on in vivo persistence, it may be that the more rapid effects of mechanical clearance masks increased survival of multicellular clusters.

MAPA encapsulation led to longer in vivo persistence of mMSCs relative to unencapsulated mMSCs, even with macrophage-mediated innate immunity and adaptive immunity clearance. The elicitation of a hostile macrophage-mediated response would presumably be reduced by the adoption of xenogen-free media for MSC culture. When injected in a protein-free buffer, MAPA-encapsulated mMSC half-life was unaffected by complement deactivation or macrophage reduction, suggesting that other mechanisms are responsible for their clearance. An adaptive immune response was elicited by injecting allogeneic hosts with mMSCs, which is consistent with prior results indicating that, despite expressing low levels of MHC molecules, MSCs still generate alloimmunization in both mice and humans (35, 36). The ability of MAPA encapsulation to partially protect alloimmunized MSCs may be useful in therapies utilizing repeated dosages of allogeneic MSCs.

A single injection of licensed, MAPA-encapsulated mMSCs significantly increased early engraftment of major MHC-mismatched BM cells in immunocompetent mice. In a prior study, MSCs have been shown to increase engraftment of allogeneic donors in sublethally irradiated hosts, but with repeated injections and a larger total dosage of MSCs than used in the present study (35). Here, a single injection at the chosen dose of unencapsulated mMSCs, even when licensed, did not increase allogeneic engraftment compared with buffer controls. The correlation between mMSC persistence at 24 h and engraftment outcome suggests that the longer retention of MAPA-encapsulated mMSCs is key to reduced donor rejection. Licensed, MAPA-encapsulated primary mMSCs also increased allogeneic engraftment compared with unencapsulated and buffer controls. Administration with licensed hMSC MAPA encapsulates, on the other hand, did not increase engraftment. Although hMSCs may exert immunomodulatory effects in murine hosts (37), cross-species incompatibility of immunomodulatory proteins may reduce the efficacy of hMSCs in mouse models. Interestingly, licensed bare hMSCs led to reduced allogeneic engraftment compared with both buffer and MAPA encapsulate administration. Xenogenic MSCs may induce stronger inflammatory responses compared with autologous and allogeneic MSCs (38), and may explain the reduced engraftment accompanying bare hMSC injection. The protective qualities of MAPA encapsulation may have physically separated hMSCs from host cells, therefore preventing a similar reduction.

As unlicensed MAPA mMSCs did not increase engraftment, licensing was likely necessary to elicit an immunomodulatory phenotype in mMSCs. Irradiation increases TNF α and IFN- γ in peripheral blood, but at an order of magnitude lower than concentrations typically used to license MSCs (39). TNF α and IFN- γ exposure appeared to override the differences in gene expression among mMSCs cultured on tissue culture plastic, as multicellular clusters in unmodified microgels, and as MAPA encapsulates, which themselves are likely a result of cellularity and growth substrate differences (19, 40). However, in response to licensing, encapsulates in purely alginate microgels displayed increased up-regulation of immunomodulatory genes compared with those in APA microgels. The additional cross-linking with PDL would likely have decreased substrate viscoelasticity, which has been linked to a more muted response to licensing in encapsulated MSCs (41). Nevertheless, the ability of MAPA mMSCs to broadly adopt an immunomodulatory phenotype upon licensing supports their usage to reduce dosing and increase efficacy.

The results of this study indicate that biomaterial encapsulation of mMSCs into MAPA microgels substantially increases in vivo retention, even with innate and adaptive immune clearance mechanisms; and that encapsulated mMSCs could respond to inflammatory cytokines. Ultimately, this strategy increased the immunomodulatory mMSC effects in a model of allogeneic BM transplantation. The work here may lead to improvements in MSC therapies by reducing dosing and enhancing MSC resistance against

immune clearance, potentially enhancing outcomes in disease contexts that benefit from MSC administration.

Materials and Methods

For additional methods, see *SI Appendix*.

Alginate Preparation. Sodium alginate with molecular weight of 139 kDa was purchased from FMC Biopolymer and modified as previously described (17).

Encapsulation and Microgel Modification. Encapsulation technology was adapted from refs. 17 and 42.

Mice. All animal experiments were performed in accordance with institutional guidelines and approved by the Institutional Animal Care and Use Committee of the Faculty of Arts and Sciences at Harvard University.

In Vivo Residence Time. A total of 1.0×10^5 MSCs expressing firefly luciferase was injected either with or without encapsulation.

BM Transplant. Recipient BALB/c mice received 700 rad for sublethal ablative conditioning by total body irradiation 1 d before transplantation. A total of 2.5×10^6 GFP B6 and 2.5×10^6 BALB/c BM cells were combined and injected i.v. A total of 4×10^5 MSCs was used in MSC conditions.

ACKNOWLEDGMENTS. The work was supported by the National Institutes of Health through Grants R01 EB014703 and R01 EB023287, and the Wyss Institute for Biologically Inspired Engineering at Harvard University. See *SI Appendix*.

- H. M. Lazarus, S. E. Haynesworth, S. L. Gerson, N. S. Rosenthal, A. I. Caplan, Ex vivo expansion and subsequent infusion of human bone marrow-derived stromal progenitor cells (mesenchymal progenitor cells): Implications for therapeutic use. *Bone Marrow Transplant.* **16**, 557–564 (1995).
- E.-J. Kim, N. Kim, S.-G. Cho, The potential use of mesenchymal stem cells in hematopoietic stem cell transplantation. *Exp. Mol. Med.* **45**, e2 (2013).
- A. Bartholomew *et al.*, Mesenchymal stem cells suppress lymphocyte proliferation in vitro and subsequent skin graft survival in vivo. *Exp. Hematol.* **30**, 42–48 (2002).
- P. Contreras-Kallens *et al.*, Mesenchymal stem cells and their immunosuppressive role in transplantation tolerance. *Ann. N. Y. Acad. Sci.* **1417**, 35–56 (2018).
- F. Mao *et al.*, Mesenchymal stem cells and their therapeutic applications in inflammatory bowel disease. *Oncotarget* **8**, 38008–38021 (2017).
- J. A. Ankrum, J. F. Ong, J. M. Karp, Mesenchymal stem cells: Immune evasive, not immune privileged. *Nat. Biotechnol.* **32**, 252–260 (2014).
- J. Galipeau, L. Sensébé, Mesenchymal stromal cells: Clinical challenges and therapeutic opportunities. *Cell Stem Cell* **22**, 824–833 (2018).
- K. Németh *et al.*, Bone marrow stromal cells attenuate sepsis via prostaglandin E(2)-dependent reprogramming of host macrophages to increase their interleukin-10 production. *Nat. Med.* **15**, 42–49 (2009). Erratum in: *Nat. Med.* **15**, 462 (2009).
- B. Wagner, R. Henschler, Fate of intravenously injected mesenchymal stem cells and significance for clinical application. *Adv. Biochem. Eng. Biotechnol.* **130**, 19–37 (2013).
- G. Karoubi, M. L. Ormiston, D. J. Stewart, D. W. Courtman, Single-cell hydrogel encapsulation for enhanced survival of human marrow stromal cells. *Biomaterials* **30**, 5445–5455 (2009).
- M. D. Herreros, M. Garcia-Arranz, H. Guadaluja, P. De-La-Quintana, D. Garcia-Olmo; FATT Collaborative Group, Autologous expanded adipose-derived stem cells for the treatment of complex cryptoglandular perianal fistulas: A phase III randomized clinical trial (FATT 1: Fistula advanced therapy trial 1) and long-term evaluation. *Dis. Colon Rectum* **55**, 762–772 (2012).
- N. Huebsch *et al.*, Matrix elasticity of void-forming hydrogels controls transplanted-stem-cell-mediated bone formation. *Nat. Mater.* **14**, 1269–1277 (2015).
- S. S. Ho, K. C. Murphy, B. Y. Binder, C. B. Vissers, J. K. Leach, Increased survival and function of mesenchymal stem cell spheroids entrapped in instructive alginate hydrogels. *Stem Cells Transl. Med.* **5**, 773–781 (2016).
- W. Whyte *et al.*, Sustained release of targeted cardiac therapy with a replenishable implanted epicardial reservoir. *Nat. Biomed. Eng.* **2**, 416–428 (2018).
- A. S. Lee *et al.*, Prolonged survival of transplanted stem cells after ischaemic injury via the slow release of pro-survival peptides from a collagen matrix. *Nat. Biomed. Eng.* **2**, 104–113 (2018).
- N. Huebsch *et al.*, Harnessing traction-mediated manipulation of the cell/matrix interface to control stem-cell fate. *Nat. Mater.* **9**, 518–526 (2010).
- A. S. Mao *et al.*, Deterministic encapsulation of single cells in thin tunable microgels for niche modelling and therapeutic delivery. *Nat. Mater.* **16**, 236–243 (2017).
- F. Lim, A. M. Sun, Microencapsulated islets as bioartificial endocrine pancreas. *Science* **210**, 908–910 (1980).
- T. J. Bartosh *et al.*, Aggregation of human mesenchymal stromal cells (MSCs) into 3D spheroids enhances their antiinflammatory properties. *Proc. Natl. Acad. Sci. U.S.A.* **107**, 13724–13729 (2010).
- J. Mattsson, O. Ringdén, R. Storb, Graft failure after allogeneic hematopoietic cell transplantation. *Biol. Blood Marrow Transplant.* **14** (1, suppl. 1) suppl. 1, 165–170 (2008). Erratum in: *Biol. Blood Marrow Transplant.* **14**, 1317–1318 (2008).
- R. Olsson *et al.*, Graft failure in the modern era of allogeneic hematopoietic SCT. *Bone Marrow Transplant.* **48**, 537–543 (2013). Erratum in: *Bone Marrow Transplant.* **48**, 616 (2013).
- M. Kallekleiv, L. Larun, Ø. Bruserud, K. J. Hatfield, Co-transplantation of multipotent mesenchymal stromal cells in allogeneic hematopoietic stem cell transplantation: A systematic review and meta-analysis. *Cytotherapy* **18**, 172–185 (2016).
- U. M. Fischer *et al.*, Pulmonary passage is a major obstacle for intravenous stem cell delivery: The pulmonary first-pass effect. *Stem Cells Dev.* **18**, 683–692 (2009).
- K. C. Murphy *et al.*, Measurement of oxygen tension within mesenchymal stem cell spheroids. *J. R. Soc. Interface* **14**, 20160851 (2017).
- M. D. Swartzlander *et al.*, Linking the foreign body response and protein adsorption to PEG-based hydrogels using proteomics. *Biomaterials* **41**, 26–36 (2015).
- F. Gao *et al.*, Mesenchymal stem cells and immunomodulation: Current status and future prospects. *Cell Death Dis.* **7**, e2062 (2016).
- D. Kyurkchiev *et al.*, Secretion of immunoregulatory cytokines by mesenchymal stem cells. *World J. Stem Cells* **6**, 552–570 (2014).
- T. Li, Y. Wu, Paracrine molecules of mesenchymal stem cells for hematopoietic stem cell niche. *Bone Marrow Res.* **2011**, 353878 (2011).
- S. J. Morrison, D. T. Scadden, The bone marrow niche for haematopoietic stem cells. *Nature* **505**, 327–334 (2014).
- D. Polchert *et al.*, IFN- γ activation of mesenchymal stem cells for treatment and prevention of graft versus host disease. *Eur. J. Immunol.* **38**, 1745–1755 (2008).
- A. I. Pravydyuk, Y. A. Petrenko, B. J. Fuller, A. Y. Petrenko, Cryopreservation of alginate encapsulated mesenchymal stromal cells. *Cryobiology* **66**, 215–222 (2013).
- G. Orive, S. K. Tam, J. L. Pedraz, J. P. Hallé, Biocompatibility of alginate-poly-L-lysine microcapsules for cell therapy. *Biomaterials* **27**, 3691–3700 (2006).
- A. Martinsen, G. Skjåk-Braek, O. Smidsrød, Alginate as immobilization material: I. Correlation between chemical and physical properties of alginate gel beads. *Bio-technol. Bioeng.* **33**, 79–89 (1989).
- Z. Cesarz, K. Tamama, Spheroid culture of mesenchymal stem cells. *Stem Cells Int.* **2016**, 9176357 (2016).
- A. J. Nauta *et al.*, Donor-derived mesenchymal stem cells are immunogenic in an allogeneic host and stimulate donor graft rejection in a nonmyeloablative setting. *Blood* **108**, 2114–2120 (2006).
- M. E. Reinders *et al.*, Safety of allogeneic bone marrow derived mesenchymal stromal cell therapy in renal transplant recipients: The neptune study. *J. Transl. Med.* **13**, 344 (2015).
- D. J. Prockop, J. Y. Oh, R. H. Lee, Data against a common assumption: Xenogenic mouse models can be used to assay suppression of immunity by human MSCs. *Mol. Ther.* **25**, 1748–1756 (2017).
- J. H. Pigott, A. Ishihara, M. L. Wellman, D. S. Russell, A. L. Bertone, Investigation of the immune response to autologous, allogeneic, and xenogeneic mesenchymal stem cells after intra-articular injection in horses. *Vet. Immunol. Immunopathol.* **156**, 99–106 (2013).
- R. Sakai *et al.*, Effect of sublethal total body irradiation on acute graft-versus-host disease and graft-versus-leukemia effect in SCID mice. *Bone Marrow Transplant.* **20**, 183–189 (1997).
- M. Darnell *et al.*, Material microenvironmental properties couple to induce distinct transcriptional programs in mammalian stem cells. *Proc. Natl. Acad. Sci. U.S.A.* **115**, E8368–E8377 (2018).
- K. H. Vining, A. Stafford, D. J. Mooney, Sequential modes of crosslinking tune viscoelasticity of cell-instructive hydrogels. *Biomaterials* **188**, 187–197 (2019).
- P. S. Lienemann *et al.*, Single cell-laden protease-sensitive microniches for long-term culture in 3D. *Lab Chip* **17**, 727–737 (2017).